

A Global EMC-FDTD Simulation Tool for High-Frequency Carrier Transport in Semiconductors

K. J. Willis, S. C. Hagness, and I. Knezevic
Department of Electrical and Computer Engineering
University of Wisconsin-Madison
Madison, WI 53706, USA
e-mail: kjwillis@wisc.edu

Abstract—We present a computational tool for the characterization of conductive media at THz frequencies. By coupling the Ensemble Monte Carlo (EMC) simulator of carrier dynamics and the finite-difference time-domain (FDTD) solver of Maxwell's equations, we develop and characterize a robust and versatile global simulator that interactively tracks field-particle dynamics. In this report the EMC-FDTD simulator is used to model the interaction of bulk doped silicon with THz frequency electromagnetic plane waves. The performance of the simulation tool is investigated in terms of several simulation parameters, including grid cell size and carrier ensemble size. The complex conductivity of doped silicon at THz frequencies obtained from the combined EMC-FDTD solver is in good agreement with available experimental results.

INTRODUCTION

The plasma frequency and characteristic scattering rate of doped semiconductors are typically in the terahertz (THz) frequency range. For this reason, the THz-frequency materials characteristics of doped semiconductors cannot be well described by models used in the microwave or optical regimes. In the THz regime, time-domain spectroscopy (TDS) has been used to estimate the conductivity of doped silicon for several doping densities [1]. The experimental data was well fit by a Cole-Davidson conductivity model, but that model is limited in applicability to the specific doping densities of that study.

Numerical characterization of carrier transport in semiconductors via the typical Ensemble Monte Carlo (EMC) implementation is limited by the quasistatic assumption inherent to the Poisson's equation solver. As the frequency of the stimulating electromagnetic wave or AC electronic signal

approaches the THz regime, this quasistatic assumption loses validity and fully electrodynamic field calculations are required to ensure accuracy.

The finite-difference time-domain (FDTD) method is a fully electrodynamic, highly accurate solver based on Maxwell's curl equations [2]. Past research has explored the combined EMC-FDTD solver in the context of AC device characterization [3]–[5]. The necessary consideration of a DC electric field component requires continued Poisson's equation calculations in addition to FDTD. Simultaneous adherence to the accuracy restrictions of FDTD and the Poisson's equation solver necessitates substantial computational resources, limiting solver applicability.

In this paper we use the coupled EMC-FDTD solver to examine the interaction of high-frequency electromagnetic waves with doped bulk silicon. Propagating plane waves with no DC component are used to stimulate electron motion; the Poisson's equation solver is not necessary for this calculation. We examine simulation performance in the context of predicted conductivity convergence under variation in grid cell size, ensemble size, averaging technique, and impedance mismatch. Finally, we show good agreement between extracted material characteristics and documented experimental results for doped silicon at THz frequencies.

NUMERICAL METHOD

In the combined EMC-FDTD solver electric and magnetic fields from FDTD influence EMC carrier motion according to the Lorentz force. Microscopic currents resulting from carrier motion in

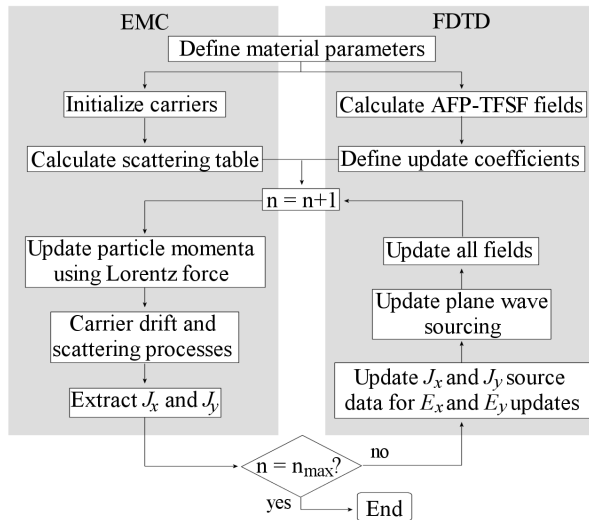


Fig. 1. EMC-FDTD global simulation flowchart. The EMC and FDTD simulations are initialized independently. The time step counter is n . Currents and fields pass between the two simulation tools at every time step.

the EMC correspondingly influence new FDTD-computed field values according to Maxwell's curl equations. The simulation flowchart in Fig. 1 shows the interaction between EMC and FDTD solvers at every time step.

For both EMC and FDTD we use two-dimensional (2D) computational domains defined in the $x - y$ plane. The EMC domain is filled with (001) doped silicon with doping density $n_0 = 10^{17} \text{ cm}^{-3}$. Typical simulation carrier ensemble size is $O(10^5)$. To permit examination of the interaction between these carriers and propagating THz-frequency electromagnetic plane waves, the EMC domain is embedded into an FDTD domain.

We assume a TE_z mode for the electromagnetic wave; thus the FDTD grid comprises E_x , E_y , and H_z field components. The FDTD simulation testbed is a semi-infinite half space of doped silicon (Regions B and C in Fig. 2) and a semi-infinite half space of air (Region A in Fig. 2). Region A is assigned a dielectric constant of 1 (and zero conductivity). A dielectric constant of 11.8 is assigned to Regions B and C. Region C is filled with an assumed value for the continuous bulk DC conductivity of doped silicon, $\bar{\sigma}$. Region B contains the embedded EMC domain; the conductivity terms in the FDTD update equations for E_x and E_y are

removed from Region B, and interaction of FDTD fields and EMC currents is enforced.

The EMC formulation accounts for the smooth materials interface by enforcing specular reflection of carriers at the left and right boundaries of the domain. The top and bottom boundaries are given periodic boundary conditions, to allow unrestricted carrier motion in the vertical direction. The FDTD domain boundaries are treated with convolutional perfectly-matched layer absorbing boundary conditions [2], allowing finite-grid representation of an infinite space. Plane waves are introduced with propagation direction normal to the interface via the analytic field propagation total-field scattered-field (AFP-TFSF) formulation [6].

Fig. 2 shows the 2D spatial distribution of the E_y phasor amplitude, extracted via discrete Fourier transform over several periods of electromagnetic wave oscillation. The field amplitude is attenuated as a function of depth in both Regions B and C. Amplitude decay in region C corresponds to that expected for dielectric with conductivity $\bar{\sigma}$. No conductivity is enforced in Region B; field decay in the coupled region results from the carrier-field interaction, exhibiting the macroscopic phenomenon of the skin effect in the coupled region.

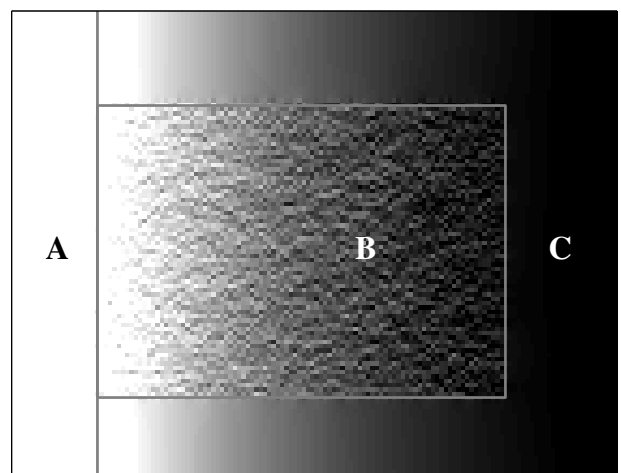


Fig. 2. Amplitude of E_y field phasor, where white corresponds to high field amplitude and black corresponds to low field amplitude. The materials interface is indicated by the vertical gray line. The section of the domain shown here lies within the AFP-TFSF boundary; an incident plane wave is sourced from the left boundary. Region B is the EMC-FDTD coupled region, whose boundary is marked by a solid gray box, and Region C is pure-FDTD doped silicon.

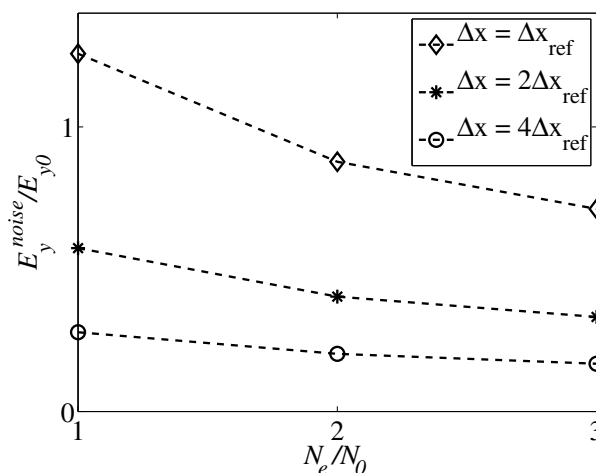


Fig. 3. Average noise of E_y in the EMC-FDTD coupled region for several values of electron ensemble size and grid cell size. E_y^{noise} is calculated as $\sqrt{\langle |E_y|^2 \rangle - \langle E_y \rangle^2}$ and is normalized by $|E_y|$ at the materials interface. $\Delta x_{ref} \approx 400$ nm is a reference grid cell size. Increasing the size of the ensemble reduces noise, as expected, but increasing the grid cell size produces a much larger improvement.

Noise in the E_y phasor amplitude in Region B is caused by EMC thermal electron motion; E_x , J_x and J_y also exhibit such minor fluctuations in phase and amplitude. To reduce the impact of this noise on conductivity calculations, spatial averages are taken over small regions surrounding each grid location in the extracted phasor quantities. These noise-reduced quantities are used in the effective linear-regime conductivity calculation: $\check{\sigma}(\omega) = \{\mathbf{E}(\omega) \cdot \mathbf{J}^*(\omega)\} / |\mathbf{E}(\omega)|^2$.

PERFORMANCE CHARACTERISTICS

Fig. 3 shows the variance of $|E_y|$ in Region B as a function of electron ensemble size N_e for several grid cell sizes Δx . Larger carrier ensembles show decreased phasor quantity noise, at the cost of an increased computational burden, as expected. Increasing Δx reduces computational burden, because of the smaller FDTD array storage and computational requirements, and Fig. 3 shows dramatic noise reduction for increased Δx . This improvement directly contrasts the EMC-Poisson solver accuracy requirements, which favor smaller grid cells for improved electrostatic calculations. The EMC-FDTD solver achieves significant noise reduction for larger Δx by including a larger body of carriers in each J_x and J_y grid point calculation. Instead of choosing several grid points per Debye

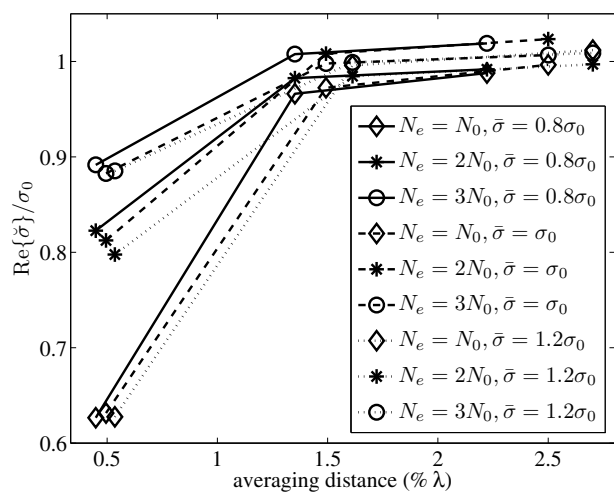


Fig. 4. Extracted conductivity with varied averaging region size, electron ensemble size, and surrounding uniform conductivity. N_0 is a reference ensemble size, typically $O(10^5)$. Larger averaging region size leads to convergence in $\check{\sigma}$. Ensemble size is associated with data marker, so that diamonds (\diamond) show data for the smallest ensemble and circles (\circ) show data for the largest ensemble. Level of impedance mismatch between Regions B and C, examined through modified $\bar{\sigma}$, is associated with line type. See text for discussion.

length, as per Poisson solver accuracy and stability requirements, the EMC-FDTD grid cell size may be defined by the much less restrictive FDTD numerical dispersion requirements, which require Δx to be smaller than roughly $1/20^{\text{th}}$ of the smallest stimulating wavelength or electromagnetic feature of interest.

Fig. 4 shows $\check{\sigma}$ as a function of phasor quantity averaging region size, for several values of ensemble size and several levels of impedance mismatch between Regions B and C. As the averaging regions size is increased, $\check{\sigma}$ converges. Increased ensemble size also leads to convergence in $\check{\sigma}$, indicating correspondence between decreased phasor quantity noise and convergence in $\check{\sigma}$. Finally, Fig. 4 allows examination of the impact of impedance mismatch between the EMC-FDTD coupled Region B and the surrounding pure-FDTD Region C. These results show $\check{\sigma}$ to be insensitive to multiple reflections within Region B resulting from impedance mismatch between Regions B and C. While $\bar{\sigma}$ may be iteratively modified between simulations to ensure good impedance matching, relaxing this requirement significantly reduces computational time.

RESULTS

We compare the complex $\check{\sigma}$ with experimental results obtained via reflecting THz-TDS [1]. The DC resistivity of the n-type doped silicon sample used is given as $8.15 \Omega\text{cm}$, corresponding to $n_0 \approx 5.5 \times 10^{14} \text{ cm}^{-3}$ [8]. This doping density is used in the EMC-FDTD solver, and the pure-FDTD bulk conductivity is modified to match.

The analytical best fit of the Cole-Davidson model to the data is given in experimental report [1]. The Cole-Davidson fit can be regarded as a faithful representation of the experimental data. Figure 5 compares the EMC-FDTD-extracted doped silicon resistivity to the best-fit to experimental results. The global solver provides results which match well to experiment. The real part of the conductivity shows excellent agreement, especially at higher frequencies. The imaginary component of the conductivity shows reasonably good agreement, even though small phase errors in the computationally and experimentally extracted conductivities would show up here. Small changes to sample position in the reflecting THz-TDS experimental setup cause spurious phase shifts in observed quantities [7]. In the numerical tests, n_0 is sufficiently low that the binary Coulomb interactions between individual carriers should not substantially contribute to the observed conductivity, but because the plasma frequency ω_p is $O(10^{12})$, plasmon scattering may be important.

CONCLUSION

This preliminary work on a combined EMC-FDTD solver demonstrates its utility in characterization of doped semiconductors at THz and sub-THz frequencies. Comparison to observed doped silicon complex conductivity has shown that this global numerical technique provides conductivity values that match well to experiment. The EMC-FDTD solver has demonstrated improved accuracy for larger Δx , in contrast to traditional EMC-Poisson accuracy requirements. The EMC-FDTD global solver shows promise as a method for full characterization of doped silicon at THz frequencies.

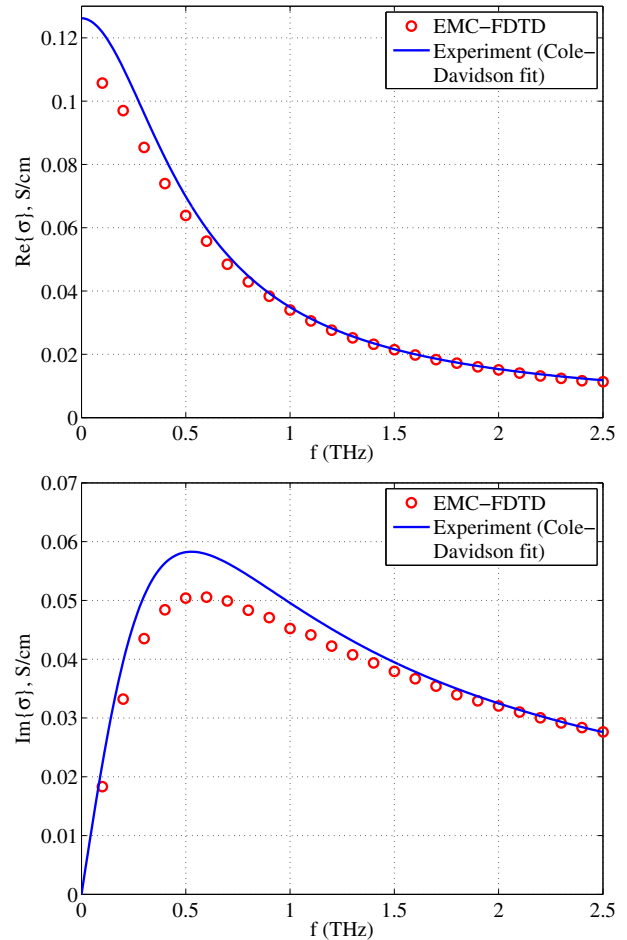


Fig. 5. THz conductivity of doped bulk silicon. The EMC-FDTD conductivity (circles) agrees well with the experimental data of Ref. [1] (presented here via a faithful Cole-Davidson analytical fit, solid curve).

REFERENCES

- [1] T. I. Jeon and D. Grischkowsky, *Phys. Rev. Lett.* Vol. 78, pp. 1106–1109, 1997.
- [2] A. Taflové and S. C. Hagness, *Computational Electrodynamics: The Finite-Difference Time-Domain Method*, Artech House, 3rd ed., 2005.
- [3] R. O. Grodin, S. M. El-Ghazaly, and S. Goodnick *IEEE Trans. Microw. Theory Tech.* Vol. 47, pp. 817-829, 1999.
- [4] J. S. Ayubi-Moak, S. M. Goodnick, S. J. Aboud, M. Saraniti, and S. El-Ghazaly *J. Comput. Electron.* Vol. 2, pp. 183-190, 2003.
- [5] J. S. Ayubi-Moak, S. M. Goodnick, and M. Saraniti, *J. Comput. Electron.* Vol. 5, pp. 415-418, 2006.
- [6] J. B. Schneider, *IEEE Trans. Antennas Propag.* Vol. 52, pp. 3280-3287, 2004.
- [7] S. Nashina, O. Morikawa, K. Takata, and M. Hangyo, *J. Appl. Phys.* Vol. 90, pp. 837-842, 2001.
- [8] R. Hull, *Properties of Crystalline Silicon* IET, 1999.